

16<sup>th</sup> Australasian Fluid Mechanics Conference  
Crown Plaza, Gold Coast, Australia  
2-7 December 2007

## Water velocity measurements inside a hydrocyclone using an Aeroprobe & Comparison with CFD predictions

M. S. Brennan<sup>1</sup>, M. Fry<sup>2</sup>, M. Narasimha<sup>1</sup>, P. N. Holtham<sup>1</sup>

<sup>1</sup>The Julius Kruttschnitt Mineral Research Centre  
University of Queensland, Isles Rd, Indooroopilly, Queensland, 4068 AUSTRALIA

<sup>2</sup>Department of Chemical Engineering  
University of Cape Town, Cape Town, SOUTH AFRICA

### Abstract

Water Velocities inside a 150mm Krebs<sup>TM</sup> DF6 classifying hydrocyclone have been measured using an Aeroprobe<sup>TM</sup>. Although the Aeroprobe disturbs the flow, the axial and tangential velocity measurements are qualitatively sensible and the integral wall pressure obtained from the measured tangential velocity profile is close to the measured wall pressure at the same elevation, which suggests that the measured tangential velocities are still reasonably accurate. The time averaged velocities from Large Eddy Simulations of the same cyclone geometry in Fluent<sup>TM</sup> are within 15% of the measured velocities.

### Introduction

#### Hydrocyclones

Classifying hydrocyclones are used extensively in mineral processing to classify mineral slurries on particle size. They are commonly used in mineral processing circuits immediately after a grinding mill where the cyclone overflow stream, which contains fine liberated material, is fed to a flotation cell and the underflow stream, which contains coarse un-liberated material, is returned to the mill for further grinding. Hydrocyclones do not classify perfectly and hence some fine material is always recycled to the mill and is subject to further unnecessary grinding, and which reduces the effective throughput of the mill. At the same time pumping the slurry through the hydrocyclone consumes energy and also wear due to abrasion by the slurry is a major maintenance cost. Improvements in any of these aspects of cyclone performance will have major cost benefits in mineral processing.

A general arrangement of a hydrocyclone is shown in Figure 1. The slurry is fed tangentially into the cyclone at the top and the circular geometry induces a swirling flow which is also usually turbulent. Classification is derived from the centripetal acceleration on particles arising from the swirl. In the outer region (near the wall) the axial velocity is downward and in the central zone the axial velocity is upward, with an axial flow reversal and flow separation near the underflow. The outlets are usually open to the atmosphere and the swirl generates a region of negative pressure which draws air in and a central axial air core forms.

Hydrocyclones are designed to cut at a particular particle diameter where particles much larger than the cut size migrate rapidly to the wall and move downward and out the underflow. Particles smaller than the cut size do not classify and tend to split between the underflow and overflow in proportion with the flow split. Particles around the cut size move towards the wall slowly in the down-flow region and so get trapped in the flow reversal in the apex and are carried up in the up-flow where they migrate back out again and so tend recirculate with a long residence time inside the device. Short circuiting of large particles to the

overflow is known to occur both around the vortex finder and near the bottom of the apex and is influenced by turbulence.

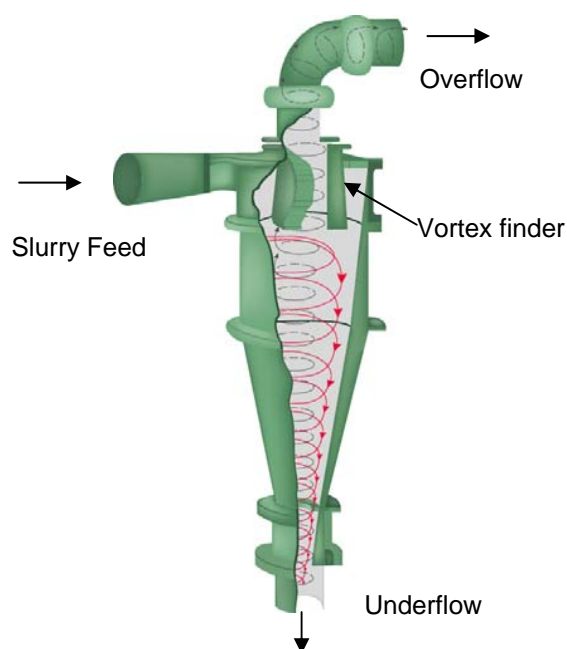


Figure 1, General arrangement of a hydrocyclone

### Computational Fluid Dynamics

Simulation of hydrocyclones by Computational Fluid Dynamics (CFD) is of interest because an accurate CFD model should be able to predict classification behaviour and could be used as a design tool. CFD modelling of hydrocyclones has been reviewed by Narasimha et al.[10] and only a number of key papers are discussed here.

The flow in a hydrocyclone is a turbulent shear flow but the swirl introduces turbulence anisotropy with the effect of damping significantly the radial turbulent momentum transfer from what might be expected from the apparent Reynolds number.  $k-\epsilon$  models assume that turbulence is isotropic and hence over predict the radial turbulent momentum transfer (ie the shear components of the Reynolds Stress tensor) and thus under predict the tangential velocities in cyclone CFD simulations (Delgadillo [4]). This has been addressed by using the Differential Reynolds stress turbulence model (DRSM) of Launder et al [9] however both Brennan [2]) and Delgadillo [4] have shown that for a 75mm diameter hydrocyclone the DRSM turbulence model under predicts the tangential velocities and that Large Eddy Simulation (LES) gives more accurate velocity predictions. Brennan [2] used

grids with between 340,000 and  $2.4 \times 10^6$  nodes, whilst Delgado [4] used a grid of 180,000 nodes.

The use of LES in CFD of hydrocyclones is however problematical. Hydrocyclones operate at velocities which are typically around  $4-8 \text{ m.s}^{-1}$ . A 75mm cyclone is only small and 1m diameter hydrocyclones operate commonly in industry. On the premise that the Reynolds number scales with diameter and applying the criteria that the grid requirements for LES scales according to the Reynolds number to the power of  $9/4$  (See Wilcox [11]) then an LES of a 1m hydrocyclone would require a grid of around  $10^{10}$  nodes. Such a grid would be computationally impractical even for simple water simulations.

This implies CFD of larger hydrocyclones will probably need to revert to RANS/DRSM simulations and that the CFD modelling will need experimental verification and possibly calibration.

#### Aeroprobe™ vs Laser Doppler Velocimetry for hydrocyclones

Point water velocities can be measured by a number of experimental techniques. Of these, Laser Doppler Velocimetry (LDV) has advantages because LDV is non-intrusive, can take measurements over a large region of a flow field and can take turbulence measurements.

The disadvantages of LDV are that an optically clear model of the geometry needs to be constructed and the work needs to be conducted in a specialist LDV facility. An optically clear model of a 1m diameter cyclone using water would be possible, but the costs associated with fabrication and setting up the model and associated pumping equipment in an LDV laboratory would be expensive. However LDV has been used successfully to measure water velocities in hydrocyclones up to 250mm in diameter. (Hsieh [7], Devulapalli [5]). This work appears to be limited to using 1D LDV and only mean velocities and mean turbulent fluctuations inside the cyclone have been obtained.

Water velocities can also be measured by a variety of intrusive probes such as hot wire and hot film anemometers, pitot tubes and multi-hole pressure probes. Intrusive probes disturb the flow and only take measurements in the vicinity of a tapping point on the boundary of the flow. Intrusive probes are also less able to resolve turbulence. However intrusive probes are simpler and much less costly than LDV and the probe can be inserted through a simple tapping port with a sealing gland on the side of the device. Intrusive probes do not need an expensive optical model and could therefore be used to take velocity measurements inside a larger scale cyclone that would be impractical to test using LDV.

In this paper we report water velocity measurements made inside a Krebs™ DF6 (150mm) hydrocyclone which is larger than the 75 mm cyclone investigated in [2]. These measurements were conducted using a Aeroprobe™ which is a multi hole pressure probe and the velocity measurements are compared with CFD predictions of water flow inside the same cyclone geometry using Fluent™ with Large Eddy Simulation.

#### The Aeroprobe™

Wire and film anemometers are comparatively fragile and unsuited to dirty flows. Pressure probes are more robust and can be cleaned if the ports block. For these reasons a 5 hole Aeroprobe was chosen for the work and tested with a view to measuring the water velocities inside hydrocyclones.

The Aeroprobe (Figure 2) operates on a similar principle to a pitot tube, but the pressure is measured at 5 different ports on the tip. This enables the probe to resolve flow direction as well as velocity magnitude and hence the velocity components of the flow can be obtained. (Bryer and Pankhurst [3] ) Manufacturing tolerances mean that multi-hole pressure probes need to be calibrated and each probe comes with a calibration lookup table. The Aeroprobe purchased for this work comes complete with a

set of pressure transducers, a data acquisition card and a computer with the measurement software and calibration table built in.

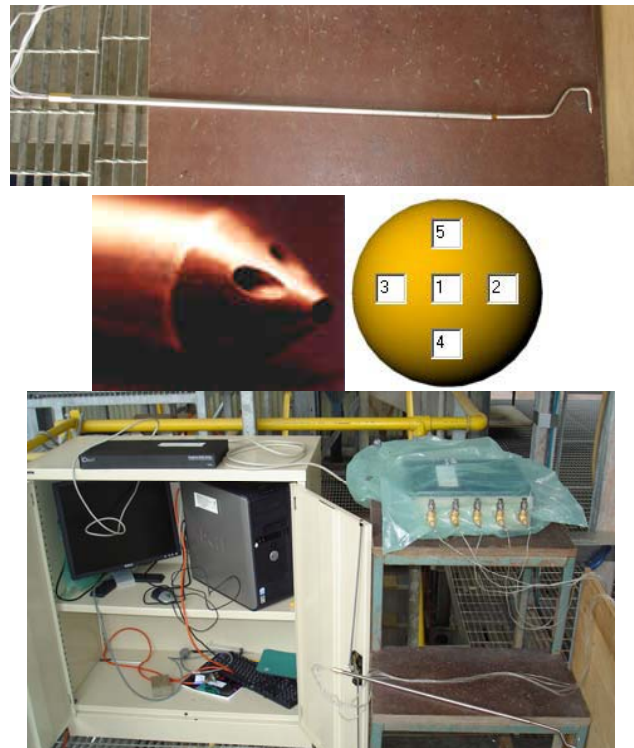


Figure 2, Views of (i) Aeroprobe, (ii) Aeroprobe tip showing pressure ports, (iii) port arrangement and (iv) Data acquisition apparatus



Figure 3, View of Krebs DF6 150 mm hydrocyclone used in velocity tests with tapping ports

#### Experimental Procedure

Figure 3 shows a view of the 150mm Krebs DF6 cyclone used for the tests. The cyclone used a 50 mm diameter vortex finder and a 25mm diameter spigot. Tapping ports were drilled into the side of the cyclone so that measurements could be taken at elevations below the top of the cyclone of 288 mm and 488 mm,

which were in the cylindrical section, and 723mm and 820 mm, which were in the apex. The cyclone was setup in a closed circuit test facility and fed with water from a sump with a variable speed pump and the overflow and underflow were returned to the sump. The feed pressure vs feed flow rate relationship for the cyclone/vortex finder/spigot combination was measured independently with a bucket and stop watch.

Each set of velocity measurements made with the Aeroprobe was taken at a set feed pressure but is reported for the equivalent feed flow rate. The probe was physically inserted into the cyclone body through the tapping port at each elevation and the tip was oriented so that the axis of the probe was horizontal. Due to the size and shape of the probe it was necessary to take measurements on the opposite side of the cyclone from the tapping port. The probe was inserted and moved manually and measurements were taken at 5mm intervals.

Preliminary measurements from the Aeroprobe using the supplied data reduction software showed a large radial velocity component. LDV measurements inside hydrocyclones by other authors [5][7] suggest that the radial velocity should be much smaller than the other velocity components.

This radial velocity was judged to be a phantom arising from the radial pressure drop induced by the swirl, which implies that the Aeroprobe measurements needed to be corrected. The correction applied here is as follows: The velocity magnitude from a pressure probe measurement is primarily calculated from the pressure at the tip port and the angle of attack is calculated from the pressure drops across the other ports. Hence the correction was applied assuming that the overall velocity magnitude and the axial component of the angle of attack were correct but the radial component of the angle of attack should be approximately zero. This assumption is only valid when the correction to the overall angle of attack is small because the overall probe coefficient is a function of the angle of attack. The assumption also intrinsically assumes that the radial velocity cannot be extracted with any reliability from the data.

The equations of motion can be simplified to show that the static pressure at the wall  $p_w$  in a hydrocyclone is the radial integral of the centrifugal acceleration induced by the tangential velocity  $u_t$ , from the air core radius  $R_a$  to the wall radius  $R_w$ :

$$p_w = \int_{R_a}^{R_w} \rho \frac{u_t^2}{r} dr \quad (1)$$

$\rho$  is the liquid phase density. The corrected tangential velocities were integrated numerically using equation (1) to determine an integral wall pressure, which was found to be within 10% of the wall pressure measured by a gauge in the tapping port at the same feed flow rate. Further the integral wall pressures at 284 mm for the two feed flow rates reported here (3.0 and 4.9 kg.s<sup>-1</sup>) were physically sensible in that they were slightly less than the pressures measured at the feed. The shape of the corrected measured tangential velocity profiles are similar to tangential velocity profiles measured in hydro-cyclones by LDV as reported in the literature [5][7]. Hence it is felt that the tangential velocities measured by the Aeroprobe with the correction described in the previous paragraph are reasonably accurate.

The uncorrected and corrected velocities for two feed water flow rates (3.0 and 4.9 kg.s<sup>-1</sup>) at three elevations below the top of the cyclone are shown on figures 4 and 5. (Dotted points) The CFD predictions (discussed below) are also shown on figures 4 and 5 (lines).

Bradley [1] discusses velocity measurements in hydrocyclones and notes that intrusive probes have been shown to disturb the flow such that the pressure drop across the cyclone is reduced at a given feed flow rate. In the case noted by Bradley [1], the

pressure drop across a 75mm cyclone was reduced by around 15% with the probe inserted. The magnitude of the flow disturbance by the Aeroprobe is still under investigation but it is felt that a disturbance of this magnitude is not sufficient to render the measurements invalid.

### CFD simulations

The CFD was conducted using Fluent™ 6.2.16. A three dimensional body fitted grid of the 150mm DF6 geometry, with a 50 mm vortex finder and 25 mm under-flow was set up in Gambit™. The geometry was based on engineering drawings supplied by Krebs and careful physical measurements of the internal dimensions of the actual cyclone used in the tests. The characteristics of the grid is listed in table 1. Water/air CFD cases were set up in Fluent at the same feed flow rates used in the two sets of velocity measurements reported here. The grid encompassed the cyclone body, overflow to the top of the vortex finder and the feed pipe up to the location of the feed pressure gauge. A water density of 994 kg.m<sup>-3</sup> and water viscosity of 0.00076 kg.m<sup>-1</sup>.s<sup>-1</sup> were used. (which was equivalent to water at an ambient temperature of 30°C.)

Grid	Cells	Radial	Tangential	Axial
A	188,465	14	60	104

**Table 1 Characteristics of grid used in CFD**

The CFD methodology was the same as reported by Brennan [2]. In summary the equations of motion are solved for a variable density and variable viscosity fluid across the entire CFD domain and the VOF model approach (Hirt and Nicols [6]), where a transport equation is solved for the volume fraction of the air phase, is used to resolve the position of the air core free surface within the CFD grid. The local volume fraction of air is used to calculate the local fluid density and viscosity. As the air and water phases are segregated, the volume fraction of air in the CFD grid will be either 0 or 1, except in a small region around the free surface.

The equations of motion were solved using the Fluent LES model with the standard Smagorinsky-Lilly [8] SGS model at a time step of 1.0x10<sup>-4</sup>s. PRESTO was used for pressure, Bounded Central Differencing was used for the momentum equation and the HRIC option was used for the air phase transport equation. Simple was used for the pressure velocity coupling. A velocity inlet boundary condition was used for the feed with the Vortex option to simulate feed turbulent fluctuations. Pressure outlet boundary conditions with an air back flow volume fraction of 1 were used at the overflow and underflow.

The Large Eddy Simulations were run to steady flow with a stable air core and the mean flow conditions and the resolved Reynolds stresses were then calculated in a user defined function by density weighted ensemble averaging over around 10<sup>4</sup> time steps.

Simulations were run at 3 and 4.9 kg.s<sup>-1</sup> feed water flow rate and with the SGS constant set to values of 0.1 and 0.2. The mean tangential and axial velocities from simulations using grid A are shown on figures 4 and 5 respectively (lines) together with experimental velocity measurements (dots) from the Aeroprobe.

Figures 4 and 5 show that the CFD predictions of the tangential velocity are generally around 15-20% greater than the velocities measured by the Aeroprobe. Increasing the value of the SGS constant from 0.1 to 0.2 improves the prediction of the tangential velocities somewhat near the peak, but worsens the predictions of the axial velocities. The wall pressures predicted by the CFD at the same elevations appear to be more than the wall pressure measured by a pressure gauge at the same feed flow rate. In fact the CFD at 4.9 kg.s<sup>-1</sup> predicts a wall pressure of 43 kPa, which is rather larger than the measured feed pressure of 35 kPa, which suggests that the CFD is in error in this situation.

Figure 6 shows the experimental feed water flow rate vs feed pressure relationship together with the feed pressures predicted by the two CFD simulations with grid A at 3.0 and 4.9 kg.s<sup>-1</sup> for the DF6 cyclone, with the 50 mm vortex finder. Figure 7 shows the contours of static pressure predicted by the CFD for the 4.9 kg.s<sup>-1</sup> case with grid A, and indicates that the wall pressure is broadly constant in the cylindrical section. Figure 6 shows that the CFD predicts feed pressures which are larger than feed pressures measured experimentally which also suggests that the CFD is over predicting the tangential velocities rather than the Aeroprobe measurements being in error because the feed pressure in a hydrocyclone is approximately equal to the sum of the pressure drop across the inlet port and the wall pressure derived from the swirl in the region between the vortex finder and the wall.

The source of error in the CFD has not been resolved properly at this point. In essence the CFD with the LES would appear to be under predicting the turbulent transfer of momentum radially across the flow, ie the CFD is predicting the flow to be less turbulent than the experiments suggest is the case. This may be because the CFD grid was too coarse and CFD simulations on finer grids are being conducted.

### Conclusions

Water velocities inside a 150 mm Krebs DF6 cyclone have been measured with an Aeroprobe. The velocity profiles are consistent with velocities measured using LDV on other hydrocyclone geometries, as reported in the literature. The integral wall pressure calculated from the measured tangential velocity profile is close to the pressure measured with a pressure gauge at the cyclone wall and at the same elevation.

CFD simulations of the same hydrocyclone geometry using Fluent with LES on a grid of 180,000 nodes predict tangential velocities which are typically 15% larger than the tangential velocities measured with the Aeroprobe. The wall pressure and feed pressures predicted by the CFD are also larger than those measured on the DF6 cyclone by pressure gauges, which would suggest that the CFD is over predicting the velocities.

### Notes

Aeroprobe is a trademark of the Aeroprobe Corporation.

Fluent and Gambir are trademarks of Ansys Inc.

Krebs is a trademark of FLSmidth Minerals Inc.

### Acknowledgments

The Aeroprobe was purchased on a University of Queensland Major Equipment and Infrastructure grant.

The Krebs DF6 cyclone was supplied by Krebs Engineers.

The experimental work for this project was conducted at the JKMRC by Matthew Fry who was an international exchange student from the University of Cape Town.

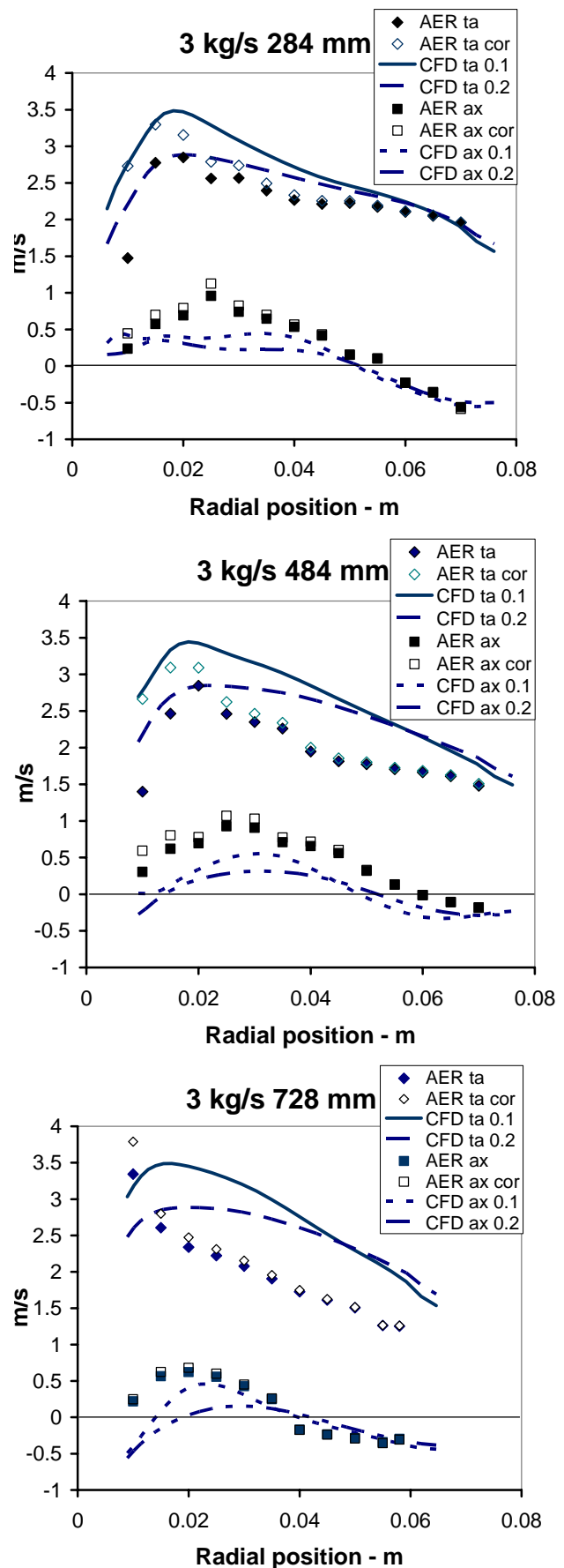


Figure 4, Velocities measured by Aeroprobe and predicted by CFD, grid A, at 3 elevations, 3 kg.s<sup>-1</sup> feed flow rate.



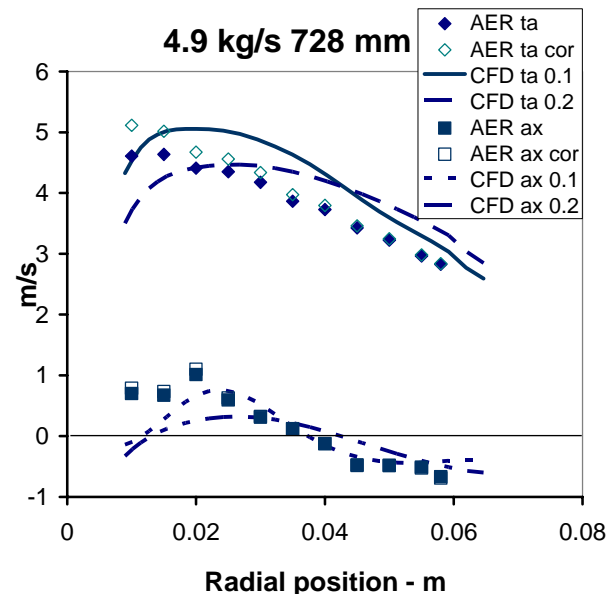
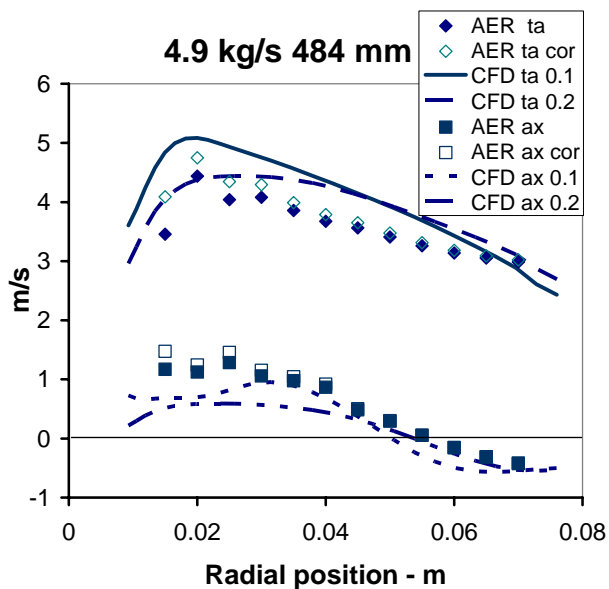
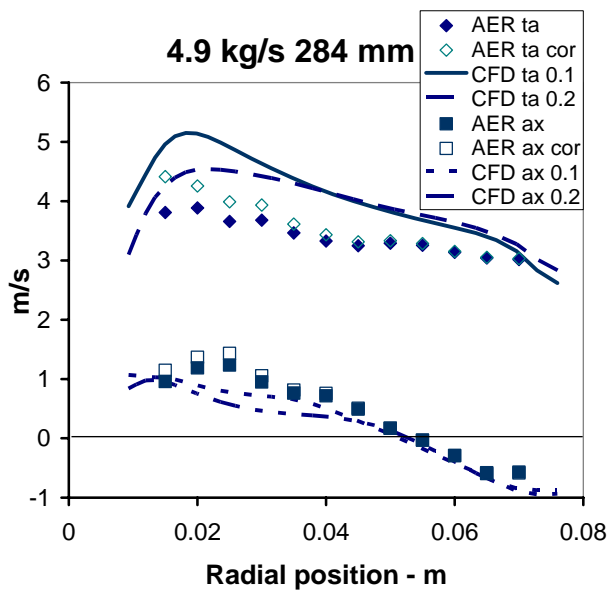


Figure 5, Velocities measured by Aeroprobe and predicted by CFD, grid A, at 3 elevations at  $4.9 \text{ kg}\cdot\text{s}^{-1}$  feed flow rate.

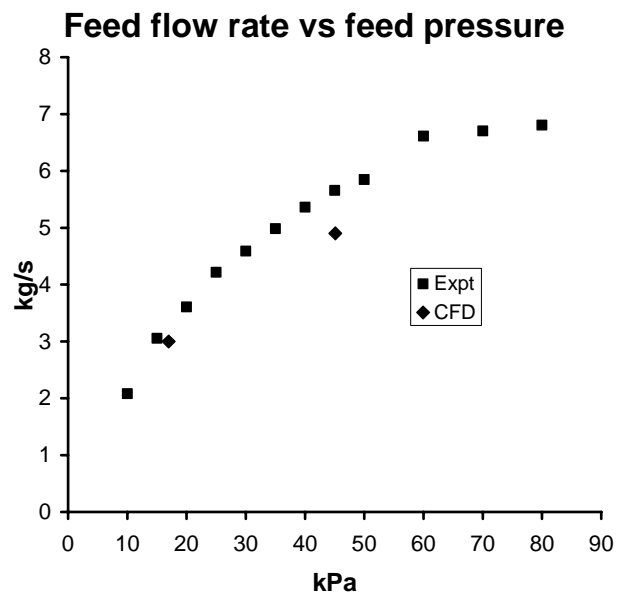


Figure 6, Experimental feed water flow rate vs feed pressure curve for DF6 cyclone and feed pressure predicted by CFD, grid A, at feed water flow rates of  $3.0$  and  $4.9 \text{ kg}\cdot\text{s}^{-1}$ .

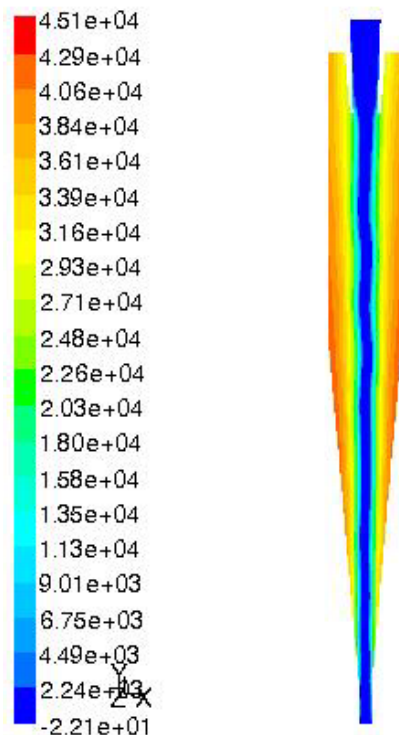


Figure 7, CFD Predicted Contours of Pressure, Grid A at  $4.9 \text{ kg}\cdot\text{s}^{-1}$

#### References

- [1] Bradley D., The hydrocyclone, Pergamon, Oxford, 1965
- [2] Brennan, M. S., CFD simulations of hydrocyclones with an air core: comparison between large eddy simulations and a second moment closure, *Chemical Engineering Research and Design*, **84A**, 2006, 495-505.

- [3] Bryer D. W., Pankhurst R. C., Pressure-probe methods for determining wind speed and flow direction, London: Her Majesty's stationery office, 1971.
- [4] Delgadillo J. A., Modeling of 75 and 250-mm hydrocyclones and exploration of novel designs using computational fluid dynamics, Ph D Thesis, University of Utah, 2006.
- [5] Devullapalli B., Hydrodynamic modelling of solid liquid flows in large-scale hydrocyclones, Ph D Thesis, University of Utah 1997.
- [6] Hirt, C. W., Nichols, B. D., Volume of fluid (VOF) method for the dynamics of free boundaries, *Journal of Computational Physics*, **39**, 1981, 201-225.
- [7] Hsieh, K. T., A phenomenological model of the hydrocyclone, Ph D Thesis, University of Utah, 1988.
- [8] Lilly, D. K., On the application of the eddy viscosity concept in the inertial subrange of turbulence, NCAR Manuscript 123, 1966.
- [9] Launder, B. E., Reece, G. J., Rodi, W., "Progress in the development of a Reynolds-stress turbulence closure", *Journal of Fluid Mechanics*, **68**, 1975 537-566
- [10] Narasimha, M., Brennan, M. S., Holtham, P. N., A review of CFD modelling for performance predictions of hydrocyclones, *Engineering Applications of Computational Fluid Mechanics*, **1**, 2007, 109-125.
- [11] Wilcox D. C., Turbulence Modeling for CFD, DCW Industries, La Canada California, 1998.